M&C 2017 - International Conference on Mathematics & Computational Methods Applied to Nuclear Science & Engineering, Jeju, Korea, April 16-20, 2017, on USB (2017)

Introduction of a Resonant Up-scattering Treatment for Multi-group Cross Section Generation

Ron Dagan*, Maarten Becker†, Aleksandar Ivanov*

*Institute for Neutron Physics and Reactor Technology, Karlsruhe Institute of Technology, Hermann-von-Helmholtz-Platz 1, 76344 Eggenstein-Leopoldshafen, Germany
†Nuclear Engineering Consultancy Dr. Maarten Becker, Lachnerstr. 15, 76131 Karlsruhe, Germany
ron.dagan@kit.edu, maarten.becker@nuc-eng.com, aleksandar.ivanov@kit.edu

Abstract - *The effect of the resonant dependent scattering kernel was previously shown to be significant for accurate criticality calculation and for the absorption rate evaluation in the resolved resonance range. However, it is not yet commonly used within deterministic codes. The current study presents first an efficient approach to include the cumulative scattering kernel into multi-group cross section data based on fine mesh flux calculation within the broad energy groups, in the vicinity of the resolved resonances. The modified scattering kernel, albeit based on the 0^{th} Legendre moment, is introduced via probability tables which are adapted to the fine mesh solver. The effect of the up-scattering is compared to Monte Carlo calculations which uses the DBRC (Doppler Broadening Rejection Correction) method. The results are in good agreement as far as the integral absorption in the investigated fuel pin and as well the spatial distribution is concerned. The slight deviations are explained to be due to the unique anisotropy characteristic of the resonant scattering which is proven by dedicated back-scattering experiments. The idea of probability tables as a replacement to the 0^{th} Legendre moment is further extended to the full double-differential scattering kernel, which accounts for the energy and angular changes of a scattered neutron after an interaction with a resonant target nucleus (^{238}U in the current study). The probability tables which are similar to the known $S(\alpha,\beta)$ probability tables in Monte Carlo allows, in principle, a Legendre moment free handling of the scattering source term in solving the transport equation by deterministic methods. This approach is important as it was shown before that the correct scattering kernel treatment calls for a very high Legendre moment order. A new treatment based on $S(\alpha,\beta)$ like probability tables provides a solution which can be regarded as equivalent to an infinite Legendre Order. Consequently, the new approach could increase the quality of deterministic solvers in the treatment of resolved resonances significantly.*

I. INTRODUCTION

The importance of the resonant up-scattering treatment on the criticality level of nuclear reactors, fuel inventory and other important effects such as the self shielding was investigated for quite a long time. Ouisloumen and Sanchez [1] showed, based on the resonant dependent formula of Blackshaw and Murray [2], that the up-scattering of neutrons, for example in the lower wing of the first main resonance of ^{238}U at 6.67 eV, can reach more than 80 % reducing considerably the resonance escape probability, as the neutrons gain energy and fall in the vicinity of the peak of the absorption resonance. The approach used by Ouisloumen and Sanchez [1] introduced the 0^{th} Legendre moment, considering an isotropic scattering in the center of mass (CoM) system. The thermal agitation of the target nuclei (i.e. ^{238}U) was approximated by a free gas model. Bouland et al. [3] used a deterministic approach to calculate the the up-scattering on the total absorption in the resolved resonance range as well as on the Doppler effect, in view of the up-scattering effect.

Later studies introduced the up-scattering effect in the vicinity of the resonances either via resonant probability $S(\alpha,\beta)$ tables [4] or via the DBRC method [5]. Both methods apply for stochastic Monte Carlo (MC) solvers. They extend the cumulative kernel mentioned above and supply equivalent results for the full double differential scattering kernel, namely the energy gain/loss of the scattered neutron as well as the scattering angle after an interaction between neutrons and resonant target nuclei. The double differential up-scattering effect was further confirmed by authors using different MC based tools, such as the GEANT, CASMO, TRIPOLI and SERPENT [6, 7, 8, 9].

Furthermore, the validity of the above up-scattering treatment was also experimentally proven for ^{238}U resonances in the RPI facility [10] and before also in the CERN laboratory for ^{232}Th [6]. Recently, a complete new approach was developed by Sanchez et al. [11]. It accounts for further possible important aspects of the up-scattering, namely the anisotropic scattering processes within the CoM. Such processes can occur at higher energies of several keV and differ to some extent from the isotropic scattering in the CoM as is done in all the above mentioned methods.

The usage of deterministic codes is still ongoing. They have their advantages over MC codes as far as issues like the computational time or the ability of complex transient solution of different kinds are concerned. For such systems, the cross section sets are based on accurate energy groups adapted to the specific type of the core under investigation. Based on the simulations performed with MC calculations it is evident that neglecting the resonant up-scattering causes for non-negligible underestimation of the absorption rate. Thereafter, the up-scattering kernel should also be applied into deterministic solvers.

Sanchez et al. [12] and Mounier et al. [13] introduced

the Doppler broadening resonant dependent kernel within the APOLLO code based on the 0^{th} Legendre moment.

The double differential scattering for multi-group deterministic solvers rely, however, in general upon higher Legendre moments that account for the energy change as well as the angle distribution after a scattering interaction. As far as the resonant up-scattering is concerned it was shown by Arbanas et al. [14] that the number of higher moments needed for the accuracy, which is reached by MC calculation, is very high and practically not realistic. On the other side, for the preparation of multi-group XS data for unit cells in infinite medium one could presume that the exact scattering angle is expected to be of a lesser importance.

In view of the above, this work introduces the resonant up-scattering treatment within a deterministic multi-group XS generation based only on the 0^{th} Legendre moment which could be integrated in leading deterministic codes, in particular, within the CENTRM code [15] which is the fine mesh solver of the known used SCALE package. The governing approach however differs, in the current study, from former ones by introducing the data, albeit equivalent to the 0^{th} Legendre moment, in a manner similar to the one used in MC calculations, namely via $S(\alpha,\beta)$-like probability tables.

Strictly speaking, one should talk as far as the 0^{th} moment is concerned only about $S(\beta)$ tables. β stands for the non-dimensional energy transfer. α includes the momentum transfer based on the angular scattering and is being actually out integrated. Those probability tables are introduced within the OZMA code [16], to analyze the effect of the energy dependent up-scattering on the resonance absorption rate in unit cells, yet allow for a significantly reduced computation time. Further, the absorption rate of the OZMA deterministic solver is compared with MC calculations, which include the fully double differential scattering kernel. A detailed analysis allows to evaluate the missing effect of the higher moments concerning the spatial shielding as well as the integrated change of the absorption rate in the whole unit cell. The comparison between the codes and treatments is performed by applying a standard reference benchmark dedicated to learn different aspects of the ^{238}U resonances, suggested by Tellier et al. [17].

A unique advantage of the deterministic probability tables procedure is the presentation of the double differential cross section. In this way, one could get an improved possibility to include the scattering source term within transport deterministic codes without the complexity of the Legendre moments, which are, regarding practical numerical issues, limited to lower order solutions. The MC-like probability tables offer an equivalent infinity Legendre order, which can comply with the needs of accuracy as mentioned in [14].

Consequently, this work presents a new treatment which can be tested against MC tools and further scattering data in form of probability tables which include the secondary energy distribution and are produced in a manner that could be suited for deterministic transport solvers leading to a solution free of Legendre moments.

II. INTRODUCTION OF THE RESONANT UP-SCATTERING INTO THE RESONANT REACTION RATES CODE OZMA

1. The OZMA code

The OZMA code [16] solves the neutron transport equation in very fine energy meshes, in particular in the resolved resonance energy range for reactor lattice unit cells, containing arbitrary mixtures of resonance nuclides. In the current study 1004 meshes were introduced for each lethargy unit. This pointwise fine flux and reaction rate calculations avoid the approximations such as the rational approximation commonly used for resonance escape probability evaluations. The enhanced accuracy obtained by the fine flux method is further free from statistical issues/problems that are inevitable by MC calculation.

As OZMA is a stand alone sophisticated resonance code and quite flexible as far as the manipulation of the group cross section is concerned, the code offers a suitable platform for the introduction of the resonant dependent scattering kernel, and it can be used as a reference analysis, which could be applied and implemented in more advanced programs such as the CENTRM code [15] of the SCALE package.

The solver option of the OZMA code used for the current study was based on the integral transport equation, computing the isotropic flux in a multi (10) region unit cell and using collision probability methods. The exclusion of the anisotropy simplifies the calculations and is in accordance with the cumulative resonant dependent scattering kernel developed by Ouisloumen and Sanchez [1].

2. Resonance dependent scattering

The resonant dependent scattering kernel includes the effect of the temperatures as well as the resonances on the differential cross section. Usually, the cross sections themselves are Doppler broadened but the scattering kernel is calculated at 0 K and with energy independent cross section. This kernel is known as the asymptotic kernel. The influence of a temperature and energy dependent kernel on the absorption rate was shown by Ouisloumen and Sanchez [1].

They introduced a modified kernel which differs strongly from the asymptotic one. Their equation is based upon Legendre moments as shown below:

$$\sigma_{sl}^{T}(E \to E') = \frac{\beta^{\star\frac{5}{2}}}{4E} \exp\left(\frac{E}{k_B T}\right) \int_0^\infty t\,\sigma_S\left(\frac{k_B T}{A} t^2\right) \exp\left(\frac{-t^2}{A}\right) \Psi_l(t)\,\mathrm{d}t \quad (1a)$$

where

$$\beta^\star = \frac{A+1}{A} \quad (1b)$$

and

$$\Psi_l(t) = H(t_+ - t)\,H(t - t_-) \int_{\epsilon_{\max}-t}^{t+\epsilon_{\min}} \exp\left(x^{-2}\right) Q_l(x,t)\,\mathrm{d}x + H(t - t_+) \int_{t-\epsilon_{\min}}^{t+\epsilon_{\min}} \exp\left(x^{-2}\right) Q_l(x,t)\,\mathrm{d}x \quad (1c)$$

and here

$$Q_l(x,t) = \frac{4}{\sqrt{\pi}} \int_0^{2\pi} \frac{p_{\mathrm{cm}}(E_C, \bar{\mu}_0^{\mathrm{cm}})}{2\pi} P_l(\bar{\mu}_0^{\mathrm{lab}})\, \mathrm{d}\phi \qquad (1\mathrm{d})$$

All other parameters are explained in [1]. The most important observation, stemming from Eq. (1), is the appearance of the energy and temperature dependent cross section σ_s within the integral over the dimensionless multiplier t of the standard neutron velocity. In addition, it is assumed that the resonant nuclide behaves like an ideal gas as far as its thermal agitation is concerned. The equation includes the influence of the resonant scattering cross section on the integrated scattering kernel and, in particular, on the up-scattering in the vicinity of the resonances. In comparison with the asymptotic kernel which evolves only down scattering, as shown in [1], the modified kernel exhibits a significant up-scattering fraction, in particular in the vicinity of the resonances which, for example, reaches 82 % of the complete scattering kernel for incident neutron with energy of 6.52 eV at the dip of the interference cross section of the main ^{238}U 6.67 eV resonance. In the current study the above isotropic resonance scattering treatment based on Eq. (1) is applied. In consequence, the Legendre moment order subscript l of Ψ_l, Q_l and P_l is zero.

III. INTRODUCTION OF THE INTEGRATED SCATTERING KERNEL INTO THE OZMA LATTICE CODE

The resolved energy range of the OZMA code is divided into a flexible number of broad energy groups which are fitted to the main resonant nuclei or to a mixture of resonant nuclides. In the current study only ^{238}U was considered as a resonant material, so the energy groups were structured to get the maximal influence of the vicinity of the resonances on the scattering procedures, avoiding numerical cutoffs due to improper group structuring. In particular, each of the first six main resonances were confined in an own dedicated energy group, where the 102.6 eV and the 116.9 eV resonances were put together between 130 eV and 101.3 eV due to their proximity on the energy scale. Further, the 66.7 eV resonance was confined within the energy limits 78.89 eV and 62.44 eV, the 36.67 eV resonance between 47.85 eV and 29.02 eV, the 20.87 eV resonances between 22.6 eV upper and 13.71 eV lower energy boundary and the 6.67 eV resonance was in a broad group between 8.315 eV and 5.043 eV. The 1004 energy points for each lethargy unit mean that in the above mentioned groups 503, 252, 252, 503 and 503 energy points were considered for each of the resonant groups respectively. The OZMA code, as mentioned in the introduction, replaces simplified approximations by accurate energy dependent treatment. This is done by the use of point-wise fine flux and external resonances profile tabulation, which are supplied at any accuracy needed, in the same manner as MC data is being prepared. Further, in this work the ENDF/B VII.1 [18] data base library was used, processed with the NJOY [19] code for the four analyzed temperatures of interest.

The OZMA code includes in the resonance range only downwards scattering. One starts with constant lethargy flux above the analyzed resolved energy range and based on the fine flux structure (as mentioned, 1004 point per lethargy unit) a downwards sweep is performed which calculates the flux from higher to lower energies. The scattering source term is based upon the classical asymptotic scattering kernel (0 K) within the slowing down theory [20]. Consequently, the flux calculation is straight forward as all the scattered neutrons are derived from energy points in which the flux was already (at higher energies) evaluated.

The calculation of the up-scattering kernel throughout the resonance energy range could be done only by an iterative process, as the contribution to energy mesh points in the domain can come not only from higher energies, where the flux is already known, but rather from lower energy points where the flux was not yet calculated (or calculated in the previous iteration). In addition, one has to note that the resonant up-scattering as well as the down scattering probabilities from each energy point to all other neighboring higher and lower energy points differ strongly from the asymptotic one. Obviously, the installed asymptotic scattering kernel in OZMA can not be further used for the relevant resonant investigated energy range.

The 0^{th} Legendre moment, as given in Eq. (1), provides the full energy distribution after a scattering interaction for each incident energy point. The scattering probabilities should be fitted to the energy point structure in OZMA to avoid mismatching and to assure detailed balance [20] and the confirmation of the current numerical treatment. Strictly speaking, for each energy point at each of the relevant resolved resonance energy groups, the upwards and downwards probabilities to all other energy points within the group must be a priori prepared. Consequently, Eq. (1) was first numerically coded, solved and the results were rewritten in form of scattering probabilities from and to neighboring energy bins for each of the above mentioned energy points within the resonance groups. Altogether, 2013 integrated S(α,β)-like probability tables were preprepared. Speaking here only about the cumulative scattering kernel, one should talk about S(β)-like probability tables, as the α-part contribution which stands for the spatial distribution is accumulated over all angles.

Based on the above, the straight forward slowing down process in the OZMA code was replaced for the isolated specific resonance energy groups by an iterative process which allowed for the insertion of cumulative scattering kernels in form of probability tables for the energy transfer after a scattering interaction. Those tables of the resonant nuclide replaced the asymptotic kernel, i.e. at each iteration, at each energy point, the integral transport equation, was solved by using contributions of the scattering source terms, from energy points above and in particular below the current point. The source term at lower energy was taken from the previous iteration. The calculation was stopped when all fluxes from two adjacent iterations at each energy point were below the convergence criteria.

IV. THE TELLIER BENCHMARK

The absorption rate calculations in view of the resonant up-scattering treatment was assessed by means of the Tellier benchmark [17]. The described pin in the benchmark includes

Table I. Geometrical dimensions of the pin cell

Zone	Radius
Fuel radius	0.409 50 cm
Cladding outer radius	0.474 36 cm
Equivalent cell radius	0.713 54 cm

Table II. Nuclide densities

Isotope	Zone	Density [b^{-1} cm^{-1}]
^{238}U	Fuel	0.021 758
^{16}O	Fuel	0.044 925
^{27}Al	Clad	0.039 220
^{16}O	Moderator	0.023 857
^{1}H	Moderator	0.047 714

only ^{238}U in the oxide fuel UO_2, which allows for a direct analysis of the resonance range without shielding of other isotopes, in particular for the S pronounced resonances of ^{238}U. The non-fuel isotopes were taken to have no resonances below 4 keV, to avoid overlapping effects on the ^{238}U resonances. This led to the chosen cladding material which was aluminum. The geometrical dimensions of the pin are given in Table I. The nuclide densities of all isotopes involved are shown in Table II.

The investigated fuel pin is divided into 10 equal volume fuel zones, which allows for an accurate estimation of the spatial and energy shielding. Beyond the 10 fuel zones the outer zones of the pin included one cladding and two moderator (water) zones.

The reference temperature chosen for the basic analysis was 900 K in accordance with power nuclear reactors. The tabulated nuclear data for all groups including the point-wise resonance cross sections was based, as mentioned above, on the ENDF/B VII.1 nuclear library.

For the effect of the scattering kernel on the absorption rate within the unit cell two calculations were performed. The reference one used the original OZMA version, namely without iteration on the flux estimation. This option calculates the scattering source term by employing the asymptotic scattering kernel for all isotopes, in particular for ^{238}U. The second calculation included the iterative process for the flux calculation, in which the asymptotic scattering kernel for ^{238}U was replaced by the prepared tabulated energy dependent cumulative scattering kernel data. The aluminum cladding, the oxygen in the fuel and in the water as well as the hydrogen were calculated by employing the asymptotic scattering kernel at the relevant energy range from 3.5 keV down to 2 eV. The up-scattering treatment was applied to the dedicated resonant groups. Between those groups within the 130 eV and 2 eV energy range the regular asymptotic treatment of OZMA was applied. The effect of the up-scattering kernel on the absorption rate over the analyzed energy range between 130 eV and 2 eV at each fuel zone is shown in Fig. 1. The average increase of the absorption rate, over the whole pin, is about 1.25 % at 900 K. The maximum increase of the absorption due to the cumulative resonant scattering kernel is at the 9^{th} ring as can be seen in Fig. 1.

It should be clarified that the absolute absorption value at the outer ring, as expected of resonance shielding, is doubled at the 10^{th} outer ring in comparison with the 9^{th} ring. The reason for the shift of the relative change to the 9^{th} ring could be explained by neutrons which are being isotropically scattered, based on the 0^{th} moment solution, and lost, albeit at the resonance energies, to the water where they are further slowed down. In the 9^{th} ring this effect is being compensated by forward scattering from the 10^{th} ring. Obviously, as the volume of the rings is equal the outer ring has the large surface with the 9^{th} ring and as the radius of the 10^{th} ring is the smallest one (2.1 mm) it enhances, to some extent, the neutrons' direct flight probability from the water to the 9^{th} ring at energies just below the resonances which eventually contribute the most to the up-scattering effect and consequently to the enhanced absorption.

In order to validate the accuracy of the deterministic approach with OZMA, the Tellier benchmark was tested with the stochastic MCNPX code [21]. The up-scattering effect was inserted into the MCNPX code via the DBRC (Doppler Broadening Rejection Correction) method [5].

This DBRC scattering treatment allows for the full angular anisotropy distribution of the scattered neutrons. By comparing two repetitive calculations with and without the scattering kernel the stochastic based full double differential scattering kernel was obtained.

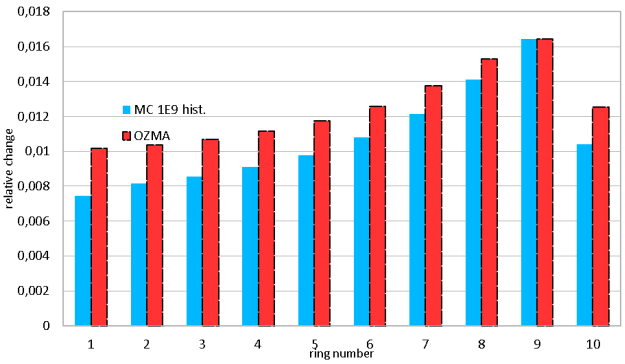

Figure 1. up-scattering effect on the absorption rate for a ^{238}U fuel pin at 900 K between 130 eV and 2 eV. The MCNPX calculations used the DBRC treatment for the double differential cross section over the entire energy range. The OZMA cumulative kernel is applied only to the 5 resonance relevant energy groups.

In this stochastic solution, all the scattering interactions for ^{238}U included the DBRC modified treatment in the whole inspected energy range between 130 eV and 2 eV. The results are shown in Fig. 1 besides the OZMA evaluation. The consistency with the OZMA based spatial distribution is considerably good. The amplitude of the OZMA results tends to be higher by about 10 % over the whole pin. The outermost and the innermost rings differ by about 20 %. Obviously, the isotropic scattering assumption near the water is expected to be stronger pronounced. The overall difference is corollary to the different numerical scattering treatment, namely cumulative kernel in OZMA vs. full scattering in MCNPX via the DBRC method. The interpretation of the two different approaches

was further illuminated by an experimental evidence based on [10]. In this experiment the scattered neutrons from ^{238}U at a back angle of 143° for different energies were counted. The experimental data was compared against the DBRC equivalent resonant treatment via S(α,β) tables [5]. The energy independent kernel used in the original MCNPX version shown with dashed line showed results which deviated by up to 80 % from the solid line MCNP with the resonant S(α,β) tables (see Fig. 2). The approach indeed fits the experimental results. In addition, Fig. 2 points out the deviations, in particular in the 10th ring due to the anisotropic scattering. The correct energy dependent scattering kernel treatment tends to increase the backward scattering of neutrons at energies just below the peak resonances. Consequently, exactly the neutrons at the lower wings of the resonance (in this case the 36.67 keV resonance) which contribute the most to the up-scattering effect are being back scattered and lost to the water as far as the absorption rate in the resonance is concerned. As this effect is included in the MC simulation either and not in the current modified OZMA version, the analyzed isotropic scattering in OZMA reduces the loss of those neutrons and consequently calculates a higher absorption rate at the outermost ring. This explanation can be also attributed to the inner rings to explain to some extent the growing differences from the 9th ring to the 1st ring. Nevertheless, one can conclude that the OZMA integrated results, in view of the deterministic isotropic approach are in considerable good agreement as long as localized effects are not accounted for. In such cases the scattering kernel near resonances possesses unique features which have mainly localized impacts as can be understood experimentally in Fig. 2. Recalling that deterministic codes are in general used for averaged group values the advantage of the OZMA modified solver is well pronounced by the computation time. It needs several seconds to calculated the results in Fig. 1 whereas, for the same accuracy and spatial distribution, the MC calculation needed with 8 processors, of the same kind as used for OZMA, one week.

V. LEGENDRE MOMENTS FREE ANGULAR SCATTERING KERNEL

The isotropic kernel which was based on the 0th Legendre moment can be extended as suggested in [1] to higher Legendre moments to include the angular effect of the scattering kernel. However, for the resonance range under investigation it was shown in [14] that a relative high number of Legendre moments is inevitable to comply with MC solutions. Consequently, it makes sense to extend the isotropic probability tables, to probability tables which in-cooperate doubled differential scattering kernel. Strictly speaking, to generate deterministic tables which could be, as the MC S(α,β) tables, equivalent to an infinite Legendre moment order. The development of such tables was numerically coded based on [22]. Eq. (2) presents the governing treatment. It uses an integral approach based on cosine bins and not on the angle itself as in the Legendre moments solution. This idea is shown on the first line of the equation where the angle transfer ($\mathbf{\Omega}' \rightarrow \mathbf{\Omega}$) is numerically replaced by a cosine bin. The scattering probabilities are being calculated based on six integrals within the

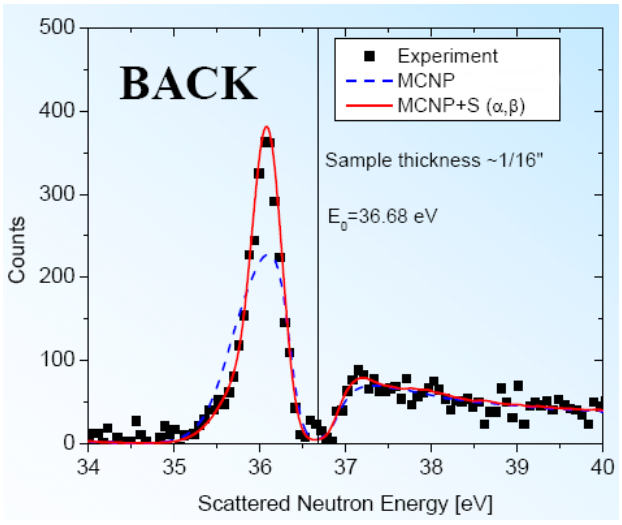

Figure 2. Comparison of neutron back-scattering at a scattering angle of 143° at 300 K. The experimental data fits well the energy and temperature dependent scattering kernel. MCNP means that the temperature dependency was included via the ideal gas assumption, but the scattering cross section was assumed to be energy independent.

c	CoM velocity
u	Neutron velocity before collision
u'	Neutron velocity after collision
μ_u	cosine of angle between the vector velocities c and u
$\mu_{u'}$	cosine of angle between the vector velocities c and u'
ϕ	azimuthal angle between the interacting and scattering planes

CoM system which are confined each time to the investigated cosine bin. The scattering probabilities are summed from all possible options within the six integrals. All the scattering options must obey the conservation law which appear in Eq. (2) as δ-functions for the relevant vector velocities. The CoM parameters in the integrals are:

$$\sigma_s^T(E \rightarrow E', \mathbf{\Omega}' \rightarrow \mathbf{\Omega}) = \frac{1}{2\pi}\sigma_s^T(E \rightarrow E', \mu_0^{\text{lab}}) \frac{1}{2\pi\nu}\left(\frac{A+1}{A}\right)^4\left(\frac{A}{\pi}\right)^{3/2} \int 2\pi u^2\,\mathrm{d}u \int \mathrm{d}\mu_u \int c^2\,\mathrm{d}c \int (u')^2\,\mathrm{d}u' \int \mathrm{d}\mu_0 u' \int \frac{2}{\sin\phi}\frac{1}{u\,v\,c}\delta\left[\mu_u - \frac{v^2 - c^2 - u^2}{2\,u\,c}\right]\frac{1}{2\,u'\,c\,K_B\,T} \frac{\delta(u'-u)}{u'^2}\exp\left[v^2 - (a+1)\left(\frac{u^2}{A} + c^2\right)\right]\delta\left[\mu_{u'} - \frac{v'^2 - u'^2 - c^2}{2\,u'\,c}\right] \frac{4\,v\,v'\,c^2}{B_0}\delta(\cos\phi - \cos\bar{\phi})\,u\sigma_s(E_r)\frac{P(u,\mu_0^{cm})}{2\pi}\,\mathrm{d}\cos\phi \quad (2)$$

The exact meaning of all other parameters can be found in [22]. Furthermore, Eq. (1) and Eq. (2) are obviously related as they depict the same phenomena. The mathematical

transformation between the two approaches was shown by Rothenstein in [23].

The numerical solution of Eq. (2) can be prepared in equi-probable bins according to the need of accuracy and the compatibility of the transferred scattering data to the transport code solver. In view of the cumulative scattering kernel used above, Fig. 3 shows graphically the double differential part, namely the angular distribution as well, based on eight bins. The contour of the graph is the first differential of the scattering cross section, namely the cumulative change of energy after a scattering interaction. The angular distribution for each scattered energy is shown for eight equal cosine bins, dividing the full cosine angle space from -1 to 1. The interacting energy is 6.52 eV which exhibits a huge part [82 %] of up-scattering as was shown in [1]. Based on the current procedure it seems that the integration of the anisotropic kernel in OZMA or in more advanced fine flux codes as CENTRM is feasible leading to MC similar accuracy, however with the advantages of deterministic codes as outlined above.

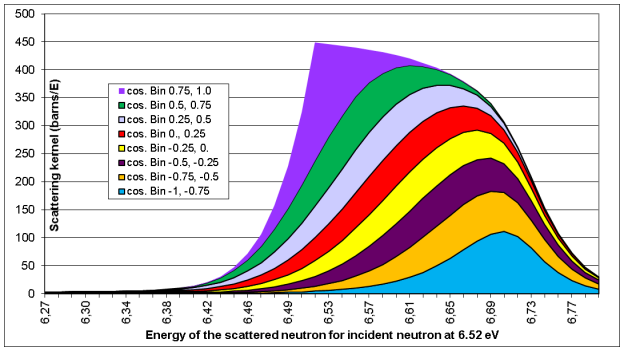

Figure 3. The double differential scattering kernel for an incident neutron at 6.52 eV. The outer contour is the cumulative kernel and the inner colored zones within it represent 8 equal cosine bins covering the whole cosine angle space from -1 to 1.

1. Influence of the deterministic solution on the Doppler effect

The impact of the deterministic up-scattering kernel on the Doppler effect in view of the OZMA solution was verified by applying more temperatures. The up-scattering effect was repeated by using data at 1200 K as well as at lower temperature 300 K and 600 K. The relative change of the Doppler effect was computed by calculating the existing Doppler effect between the mentioned four temperatures, for the case of the energy independent cumulative scattering kernel. These reference cases were then compared to the Doppler effect obtained by the insertion of the energy dependent scattering kernel. As one might expect, the changes are larger by lower temperatures. Between 300 K and 600 K the Doppler effect is increased by 7.0 % due to the modified kernel, however between 600 K and 900 K by only 2.0 % and from 900 K to 1200 K the change in the Doppler effect is 1.3 %. The up-scattering kernel contribution is, thereafter, well pronounced in the lower temperature range and it is relatively even stronger pronounced than the Doppler effect itself, which exhibit a moderate increase between 300 K and 600 K in comparison with the Doppler effect between 600 K and 900 K till 1200 K.

VI. CONCLUSIONS

The energy dependent cumulative scattering kernel was introduced into the unit cell code OZMA which solves the resonance energy range in very fine energy mesh points by using resonance profile tabulation. The replacement of the asymptotic kernel by the resonance dependent kernel was based upon the 0^{th} Legendre moment, however, presented in a new form, namely in a fine probability tabulation, matching to each mesh point of the original energy fine mesh point structure. This approach allows for a very accurate solution for the calculation of the overall resonance shielding effect. The enhanced absorption for the main 6 S resonances was about 1.28 % at 900 K and confirmed again the importance of the inclusion of the up-scattering kernel in neurotic codes and in particular also in deterministic solvers. Moreover, the integrated results over the whole pin are comparable to MC simulations where the enhanced absorption due to the DBRC [5] based up-scattering kernel was calculated to be 1.14 %, albeit where the DBRC was applied continuously to the whole energy range from 130 eV and 2 eV. In the case where only integrated results are required, the advantage of the deterministic OZMA approach over MC is evident by the far lower computation time, several seconds with one processor compared to several days by MC simulation with 8 processors. The main reason lies, among others, in the fact that the MC simulation needs for the exact shielding spatial calculation over the 10 rings about 10^9 histories. Simulations with about 10^7 histories show a biased convergence between the rings. The reliability of the OZMA calculation allowed further, by comparing to MC calculations, to estimate the importance of the full double differential scattering kernel including the angular distribution. The differences at the outer ring, between the cumulative kernel (OZMA) and the double differential energy and temperature dependent scattering kernel (MCNPX), as well as the slightly growing deviations towards the middle of the pin were explained by the enhanced back scattering, at energies just below the main resonances which are the main cause of the enhanced absorption. This effect was confirmed by dedicated experiments performed at the RPI laboratory [10]. The experimental confirmation encouraged the idea to extend the cumulative scattering probabilities to a form including the double differential scattering kernel on a level that is used in MC calculation, namely the $S(\alpha,\beta)$ scattering tables. Strictly speaking, to abandon the use of very high numbers of Legendre moments which can be quite cumbersome to implement up to a certain order number, yet are inevitable when very high accuracy is mandatory as presented by Arbanas et al. [14]. The suggested extended probability tables provide actually an infinite-like Legendre moment order, however have to be presented in form of cosine bins as shown in this study. It should be mentioned that in the case of the MC $S(\alpha,\beta)$ scattering tables, the differential scattering data is given in form of cosine bins as well, in which the scattering angle is implicitly averaged within each bin. In MC simulations one

uses up to 16 cosine bins which allow for a very good spatial distribution representation. For the deterministic case the cosine bins introduction will depend on the transport solver. The different sensitivity of the Doppler effect with and without the inclusion of the temperature dependent up-scattering kernel calls for further temperature dependent experiments beyond the room temperature experiments that were performed in RPI [10]. High temperature based experiments would extend the knowledge of the spatial resonance shielding as well as the energy shielding as was shown in current study. Such experiments at higher temperatures are envisaged in the European Institute for Reference Materials and Measurements (IRMM) at the GELINA facility in Geel.

REFERENCES

1. M. OUISLOUMEN and R. SANCHEZ, "A Model for Neutron Scattering Off Heavy Isotopes That Accounts for Thermal Agitation Effects," *Nuclear Science and Engineering*, **107**, *3*, 189–200 (1991).
2. G. L. BLACKSHAW and R. L. MURRAY, "Scattering Functions for Low-Energy Neutron Collisions in a Maxwellian Monatomic Gas," *Nuclear Science and Engineering*, **27**, *3*, 520–532 (1986).
3. O. BOULAND, V. KOLESOV, and J. ROWLANDS, "The effect of approximations in the energy distributions of scattered neutrons on thermal reactor Doppler effects," in J. DICKENS, editor, "Proceedings of the international conference nuclear data for science and technology," (1994), vol. 2.
4. R. DAGAN, "On the use of S(α,β) tables for nuclides with well pronounced resonances," *Annals of Nuclear Energy*, **32**, *4*, 367 – 377 (2005).
5. B. BECKER, R. DAGAN, and G. LOHNERT, "Proof and implementation of the stochastic formula for ideal gas, energy dependent scattering kernel," *Annals of Nuclear Energy*, **36**, *4*, 470 – 474 (2009).
6. F. GUNSING, E. BERTHOUMIEUX, G. AERTS, and 119 OTHERS, "Measurement of Resolved Resonances of ^{232}Th (n,γ) at the n_TOF Facility at CERN," *Physical Review C*, **85**, *6* (2012).
7. D. LEE, K. SMITH, and J. RHODES, "The impact of 238U resonance elastic scattering approximations on thermal reactor Doppler reactivity," *Annals of Nuclear Energy*, **36**, *3*, 274 – 280 (2009), {PHYSOR} 2008.
8. A. ZOIA, E. BRUN, C. JOUANNE, and F. MALVAGI, "Doppler broadening of neutron elastic scattering kernel in Tripoli-4®," *Annals of Nuclear Energy*, **54**, 218 – 226 (2013).
9. J. LEPPÄNEN, "Serpent - a Continuous-energy Monte Carlo Reactor Physics Burnup Calculation Code," User's manual, VTT Technical Research Centre of Finland (2015).
10. T.-I. RO, Y. DANON, E. LIU, D. P. BARRY, and R. DAGAN, "Measurements of the Neutron Scattering Spectrum from ^{238}U and Comparison of the Results with a Calculation at the 36.68 eV Resonance," *Journal of the Korean Physical Society*, **55**, *4*, 1389 (2009).
11. R. SANCHEZ, A. PREVITI, and D. MOSTACCI, "New derivation of Blackshow-Murrays formula for the Doppler-broadened scattering kernel and calculation of the angular moments via Lagrange interpolation," *Annals of Nuclear Energy*, **87, Part 2**, 113 – 125 (2016).
12. R. SANCHEZ, C. HEWKO, and S. SANTANDREA, "Numerical computation of doppler-broadening in the resonance domain," in "Proceedings of the 2013 International Conference on Mathematics and Computational Methods Applied to Nuclear Science and Engineering," Sun Valley, USA (2013).
13. C. MOUNIER and P. MOSCA, "Resonant upscattering effects on 238U absorption rates," in "Proceedings of the international conference on physics of reactors (PHYSOR2014)," Japan (2014).
14. G. ARBANAS, M. E. DUNN, N. M. LARSON, L. C. LEAL, M. L. WILLIAMS, B. BECKER, and R. DAGAN, "Convergence of Legendre Expansion of Doppler-Broadened Double Differential Elastic Scattering Cross Section," in "Proceedings of the 2012 International Conference on Advances in Reactor Physics Linking Research, Industry, and Education," Knoxville, Tennessee, USA (2012).
15. M. L. WILLIAMS, M. ASGARI, and D. F. HOLLENBACH, "CENTRM: A One-Dimensional Neutron Transport Code for Computing Pointwise Energy Spectra," in "SCALE: A Modular Code System for Performing Standardized Computer Analyses for Licensing Evaluations," *ORNL/TM-2005/39, Version 5*, vol. I-III, chap. F18 (2005), available from Radiation Safety Information Computational Center at Oak Ridge National Laboratory as CCC-725.
16. J. BARHEN and W. ROTHENSTEIN, *OZMA–a Code to Calculate Resonance Reaction Rates in Reactor Lattices using Resonance Profile Tabulations*, *EPRI*, vol. NP-926, Electric Power Research Institute, Palo Alto, Calif. (1981).
17. H. TELLIER, M. COSTE, C. RAEPSAET, and C. V. DER GUCHT, "Heavy Nucleus Resonant Absorption Calculation Benchmarks," *Nuclear Science and Engineering*, **113**, *1*, 20–30 (1993).
18. M. B. CHADWICK, M. HERMAN, P. OBLOŽINSKÝ, M. E. DUNN, Y. DANON, A. C. KAHLER, D. L. SMITH, B. PRITYCHENKO, G. ARBANAS, R. ARCILLA, R. BREWER, D. A. BROWN, R. CAPOTE, A. D. CARLSON, Y. S. CHO, H. DERRIEN, K. GUBER, G. M. HALE, S. HOBLIT, S. HOLLOWAY, T. D. JOHNSON, T. KAWANO, B. C. KIEDROWSKI, H. KIM, S. KUNIEDA, N. M. LARSON, L. LEAL, J. P. LESTONE, R. C. LITTLE, E. A. MCCUTCHAN, R. E. MACFARLANE, M. MACINNES, C. M. MATTOON, R. D. MCKNIGHT, S. F. MUGHABGHAB, G. NOBRE, G. PALMIOTTI, A. PALUMBO, M. T. PIGNI, V. G. PRONYAEV, R. O. SAYER, A. A. SONZOGNI, N. C. SUMMERS, P. TALOU, I. J. THOMPSON, A. TRKOV, R. L. VOGT, VAN DER MARCK, S. C., A. WALLNER, M. C. WHITE, D. WIARDA, and P. G. YOUNG, "ENDF/B-VII.1 Nuclear Data for Science and Technology: Cross Sections, Covariances, Fission Product Yields and Decay Data," *Nuclear Data Sheets*, **112**, *12*, 2887–2996

(2011).
19. R. MACFARLANE and A. KAHLER, "Methods for Processing ENDF/B-VII with NJOY," *Nuclear Data Sheets*, **111**, *12* (Dec 2010).
20. M. M. R. WILLIAMS, *The slowing down and thermalization of neutrons*, John Wiley & Sons, Inc., New York (1966).
21. D. B. PELOWITZ, editor, *MCNPX User's Manual Version 2.7.0*, LA-CP-11-00438 (2011).
22. W. ROTHENSTEIN and R. DAGAN, "Ideal gas scattering kernel for energy dependent cross-sections," *Annals of Nuclear Energy*, **25**, *4*, 209 – 222 (1998).
23. W. ROTHENSTEIN, "Proof of the formula for the ideal gas scattering kernel for nuclides with strongly energy dependent scattering cross sections," *Annals of Nuclear Energy*, **31**, *1*, 9 – 23 (2004).